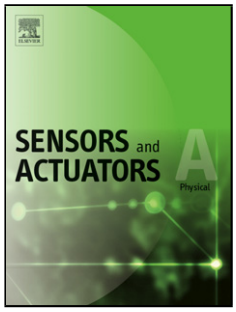

Title: Adjustable static and dynamic actuation of clamped-guided beams using electrothermal axial loads

Authors: N. Alcheikh, S. Tella, M.I. Younis

PII: S0924-4247(17)31776-4
DOI: https://doi.org/10.1016/j.sna.2018.01.066
Reference: SNA 10621

To appear in: *Sensors and Actuators A*

Received date: 6-10-2017
Revised date: 17-1-2018
Accepted date: 31-1-2018

Please cite this article as: Alcheikh N, Tella S, Younis MI, Adjustable static and dynamic actuation of clamped-guided beams using electrothermal axial loads, *Sensors and Actuators: A Physical* (2010), https://doi.org/10.1016/j.sna.2018.01.066

Adjustable static and dynamic actuation of clamped-guided beams using electrothermal axial loads

N. Alcheikh, [1] S. Tella, [1] and M. I. Younis[1, 2,a]
[1]*Physical Science and Engineering Division, King Abdullah University of Science and Technology, Thuwal, 23955-6900, Saudi Arabia*

[2]*Department of Mechanical Engineering, State University of New York, Binghamton, NY 13902, USA*

HIGHLIGHTS

- A wide-range tunable resonator and high displacement actuators are demonstrated theoretically (Finite element) and experimentally by using electrothermally actuated MEMS clamped-guided arch beams with the flexibility of shifting and choosing the operating frequency range upon demand.
- We demonstrated eight possibilities of new static and dynamic behavior resulting into different resonance frequencies and static displacement curves.
- Resonators have been designed as clamped-guided microbeams with electrothermal actuators of U-shaped structures on the sides.
- We experimentally demonstrated that the device can be used as a resonant logic gate, with active resonance tuning, showing fundamental 2-bit logic functions, such as AND,XOR, and NOR.

ABSTRACT

The paper presents adjustable static and dynamic actuations of in-plane clamped-guided beams. The structures, of variable stiffness, can be used as highly tunable resonators and actuators. Axial loads are applied through electrothermal U-shaped and flexure beams actuators stacked near the edges of curved (arch) beams. The electrothermal actuators can be configurred in various ways to adjust as desired the mechanical stiffness of the structures; thereby controlling their deformation stroke as actuators and their operating resonance frequency as resonators. The experimental and finite element results demonstrate the flexibility of the designs in terms of static displacements and resonance frequencies of the first and second symmetric modes of the arches. The results show considerable increase in the resonance frequency and deflection of the microbeam upon changing end actuation conditions, which can be promising for low voltage actuation and tunable resonators applications, such as filters and memory devices. As case studies of potential device configurations of the proposed design, we demonstrate eight possibilities of achieving new static and dynamic behaviors, which produce various resonance frequencies and static displacement curves. The ability to actively shift the entire frequency response curve of a device is desirable for

[a] Corresponding author Electronic mail: Mohammad.Younis@kaust.edu.sa

several applications to compensate for in-use anchor degradations and deformations. As an example, we experimentally demonstrate using the device as a resonant logic gate, with active resonance tuning, showing fundamental 2-bit logic functions, such as AND,XOR, and NOR.

1. Introduction

Microelectromechanical systems (MEMS) resonators and actuators based on axially loaded microbeams have been investigated widely for many applications, such as pressure sensors [1], filters [2,3], memory elements [4], logic gaits [5], signal processing [6], sensors [7], and accelerometers [8]. Most of these applications require high frequency tunability and/or high displacement. Practically, there are many factors affecting the static and dynamic responses of the devices, such as temperature variations and in-use needs, which require active compensation and tuning. Therefore, a key challenge is to develop mechanisms that enable large actuation range and at the same time high frequency tunability. Examples of such based on axial load actuation have been recently reported [9-13].

Electrothermal actuation has been widely used to tune the resonance frequency of resonators. Remtema and Lin [14] showed the decrease of the resonance frequency of an electrothermally heated microbeam by 6.5%. Hajjaj et al. [15] demonstrated experimentally and theoretically, using both analytical and finite element models, a 64% decrease and 66% increase of the resonance frequency of an electrothermally clamped-clamped straight beam before and after buckling, respectively. The finite element model was based on 3D multi-physics finite-element simulation using COMSOL. In another work [16], an electrothermally clamped-clamped arch beam was shown to have an increase in its first resonance frequency by 168%.

The most widely used electrothermal micro-actuators are the U-shaped structures [17, 18], V-shaped or Chevron shaped beams [19], and Z-shaped structures [20,21]. The V and Z shaped structures have been widely used due to their high output force (in the order of mN) and reasonable displacement (a few μm). To investigate their performance, these actuators have been simulated using finite element techniques. Using ANSYS Multiphysics, a coupled-field finite element model involving electric, thermal and mechanical fields has been utilized [20]. The results showed that these structures may have high mechanical stiffness; which limits their actuation bidirectionally and may increase the required thermal voltages for their operations. Teopoyoti –Torres et al. [22] optimized the Z-actuators based on a finite element model. The results show 50 % increases in the displacement compared to V-shape actuators. U-shaped structures are also commonly used electrothermal microactuators. These actuators are operated by utilizing asymmetrical thermal expansions of two beams with different thickness to generate displacement [23]. Yan et al. [24] introduced a new micro electro-thermal U-actuator with bidirectional vertical motion. To show the deflection and effects of the design parameters on the actuator performance, finite element simulation is carried out using Coventorware. In this simulation, three different physical domain boundary conditions, electrical, thermal and mechanical, are applied.

In a recent work [10], we presented controlling the stiffness of clamped–guided beams through V-electrothermal actuators near the beams anchors. Tunability up to 40 % for the first mode was demonstrated experimentally and numerically using a finite element model, with a midpoint displacement up to 2.5 micron for a voltage load of 5 V. The design however showed low mid-point displacement and low control over the frequency response of the device. A single device with extended static displacement range and large frequency tunability among its vibration modes has not yet been reported and is highly desirable.

In this paper, an electrothermally actuated device with high displacement, high tunability, and high frequency control is demonstrated. To achieve this, an in-plane clamped-guided arch microbeam is connected with two flexures beams and four U-structures. These actuators, being at the beam anchors, serve as variable stiffness elements and provide various electrothermal actuation schemes. Also we demonstrate the ability to actively shift the entire frequency and static displacement curves. This device can be used in applications requiring active frequency tunning and shifting. As an example, we experimentally demonstrate a resonant logic device [25] with the capability to perform the fundamental 2-bit logic functions of AND, XOR, and NOR.

2. Background

When subjecting a shallow arch to a compressive axial load, its stiffness can increase or decrease depending on whether the increase in its curvature, which increases its stiffness, can overcome the stiffness reduction from the compressive stress [26]. Here, we consider a clamped-guided arch microbeam, Fig. 1(a), and apply compressive axial loads through electrothermal actuation. For small values of initial rise, increasing the compressive axial loads leads to an initial decrease in its first resonance frequency until it reaches a critical point, after which it increases due to the increase in curvature level that dominates the compressive force effect, Fig. 1(b). The third resonance frequency on the other hand experiences a continuous decrease. By changing the stiffness on the anchor of the beam, for instance by introducing additional spring elements K_i (i=1…n), new static and dynamic behaviors can be achieved resulting into different resonance frequencies and static displacement curves. The concept is illustrated in Fig. 1(b). In this work, we aim to achieve such behaviors by utilizing the flexures thermal beams and the U-shaped thermal actuators at the edges of the beams and by actively changing the stiffness of these actuators through the electrothermal voltages. The ability to actively shift the entire frequency response curve of a device is desirable in applications to compensate for in-use anchor degradations and deformations.

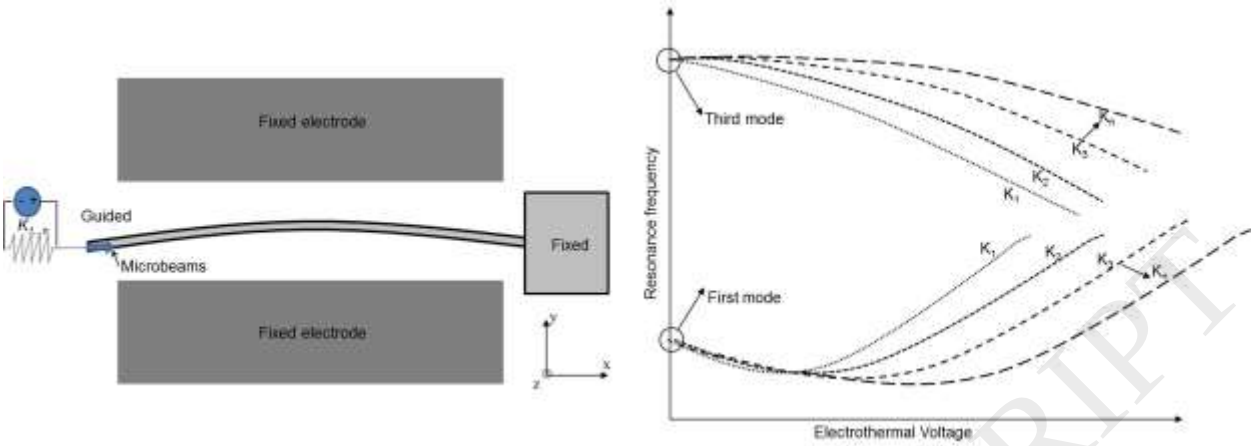

(a) (b)

Fig. 1. (a) Schematic of a clamped-guided arch beam with variable stiffness elements K_i (i=1…n). (b) Schematic illustrating the various responses of the first and third resonance frequencies while changing the stiffness coefficient.

3. Design and Device Principle

A schematic of the designed structure is shown in Fig.2(a). The variable elastic elements on the guided side of the clamped-guided arch microbeams are realized through two flexures beams and four U-shaped structures, which all act as electrothermal actuators. When any of these actuators is powered, its elastic stiffness changes depending on the applied voltage. The impact of this boundary stiffness change on the beam can be viewed as changing the initial axial pre-stress of the beam. Hence each actuator represents a variable spring element that can be configured with other actuator elements to achieve various stiffness values at the edge of the arch beam. Schematics illustrating the mechanical and electrical effects of the U-shaped structures and the flexures beams are shown in Figs. 2 (b) and 2(c), where these structures correspond to stiffness and resistance elements denoted respectively by K_A, K_B, K_C, K_D , K_E and $R_{1,2}$, $R_{3,4}$, $R_{5,6}$, $R_{7,8}$, $R_{9,10}$. To induce compressive axial loads, the U-shaped structures are electrically connected in series. In this case, the thin (hot) arm of the U actuator will be heated more than the thick (cold) arm, and hence induces deflection in the positive 'x' direction (Fig.2(a)). To achieve bi-directional motion (tensile and compressive), the structures can be electrically connected also in parallel. However, in this work, we will demonstrate only one-directional motion for the compressive axial loads.

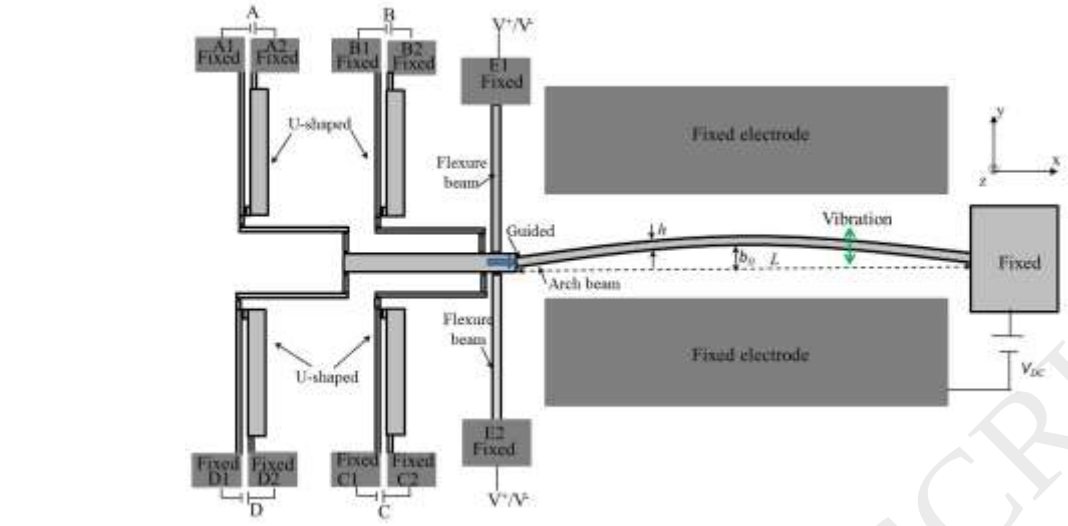

(a)

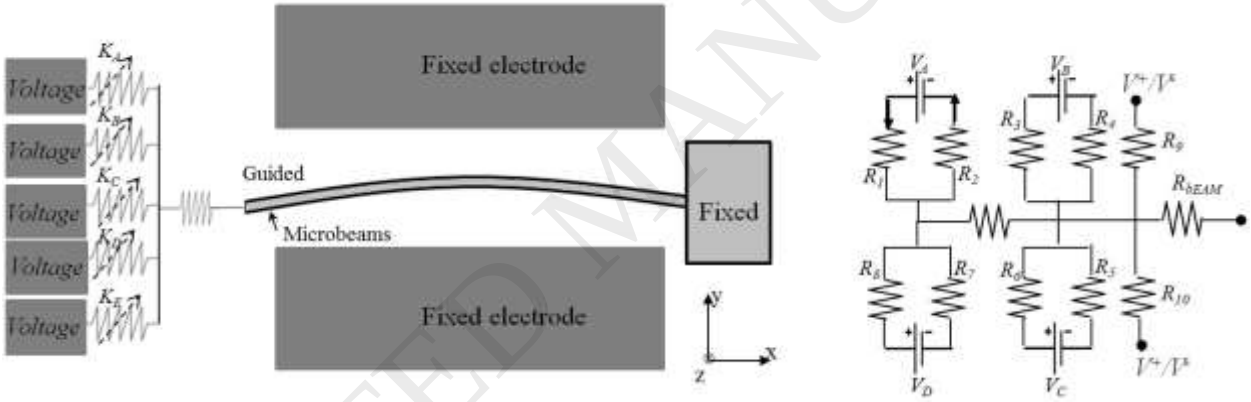

(b) (c)

Fig. 2: (a) Schematic of the structure. A fixed-guided microbeam suspended by four U-shaped structures and two flexure beams with electrothermal actuation (b) Schematic of the mechanical equivalence of the electrothermal actuators as stiffness elements denoted by K_A, K_B, K_C, K_D , K_E. The arrows denote variable stiffness elements. (c) The electrical equivalence of the device as resistance elements, including those of the electrothermal actuators and flexures denoted by $R_{1,2}$, $R_{3,4}$, $R_{5,6}$, $R_{7,8}$, $R_{9,10}$.

As shown in Fig. 2, there are eight actuation pads labeled on the U-shaped structures A1, A2, B1, B2, C1, C2, D1, and D2, and two pads on the flexure beams, which offer more than 61ways of electrical connections ($2^n - n/2$; n even), and hence electrothermal actuation combinations. Each way will result also in a different effective stiffness of the actuators. Eight cases are investigated in this paper, Fig. 3 and Table 1: Case 0 (A-B-C-D), Case 1 (B - C), Case 2 (A-D), Case 3 (A-B), Case 4 (C-D), Case 5(B-C-D), Case 6 (A-B-C-D-E1(V^+)- E2(V^+)), and Case 7 (A-B-C-D-E1(V^+)- E2(V^-)). In each case, the actuators (A, B, C, D) are activiated by powering their pads with a voltage source, as indicated in Figure 2c. For example, Case 1 (B-C) refers to activation of actuators B and C. For Case 7 (A-B-C-

D-E1(V^+)- E2(V^-)), the pads A, B , C and D are powered by connecting them to the same source voltage, and the flexure beams are powered by connecting Pad E1 with V^+ and Pad E2 with V^-. The rest of cases can be investigated depending on the desired applications. The in-plane clamped-guided microbeams are designed as arc beams. To induce vibration, they are excited electrostatically by a DC polarization voltage of 40 V and an AC harmonic load of 20 mV.

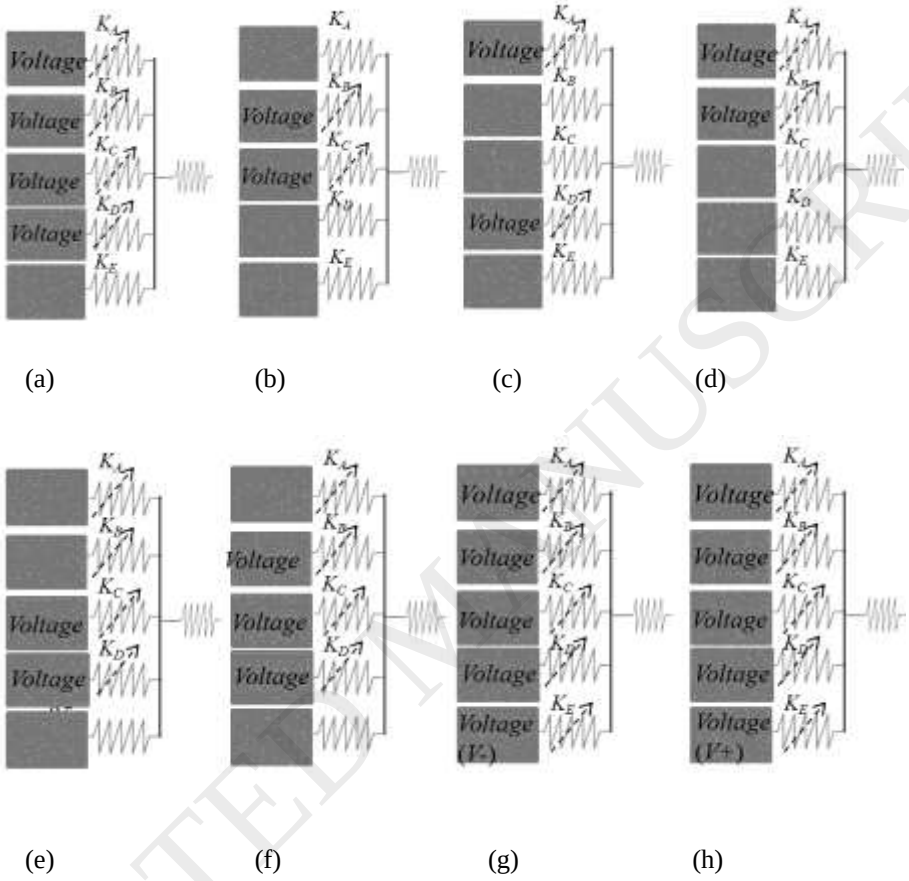

Fig. 3: Schematic illustrating the mechanical effect of the electrothermal actuators as elastic stiffness elements. (a) Case 0 (b) Case 1 (c) Case 2 (d) Case 3 (e) Case 4 (f) Case 5 (g) Case 6 and (h) Case 7. The arrows denote variable stiffness elements.

Table 1. The electrical connections of the eight studied cases.

Case	0	1	2	3	4	5	6	7
Inputs connected to the voltage source	A-B-C-D	B-C	A-D	A-B	C-D	B-C-D	A-B-C-D-E1$^-$/E2$^-$	A-B-C-D-E1$^+$/E2$^+$

The structures are fabricated from a highly conductive silicon device layer of silicon-on-insulator (SOI) wafer from MEMSCAP [27]. Fig. 4 shows a picture of one of the fabricated devices of 800µm arch beam length. The beam is 2µm in width and 25µm in depth. The gap between the actuating electrode and the beams is 10µm at the clamped ends. The gap at the mid-point is 12.5µm due to the initial curvature of 2.5µm.

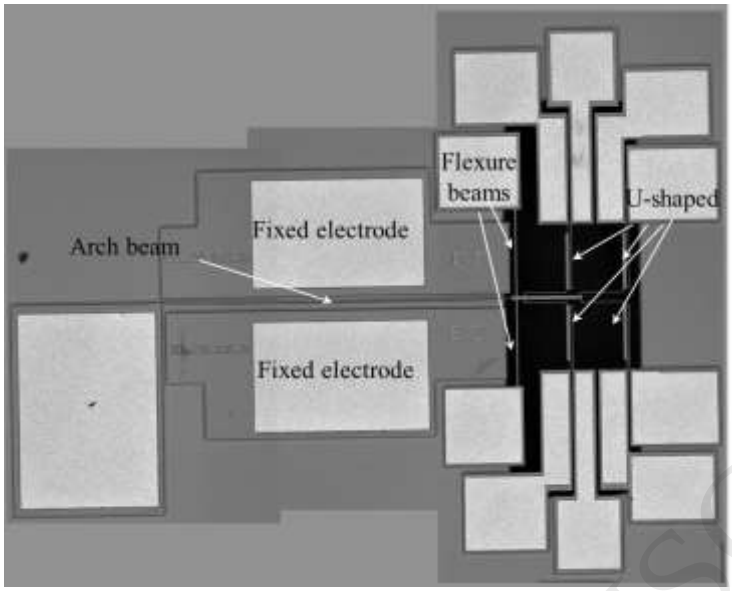

Fig. 4: A top view picture of one of the fabricated devices showing the various actuation pads (in white) used to excite the arch into vibrations and those used for the flexure beams and U-shaped actuators.

4. Finite Element Model

A multi-physics finite element FE model is built in COMSOL [28] to design the devices and to simulate their frequency and static responses before fabrication. To take into account the various physical domains, various solvers have been utilized, which include the Solid Mechanics, Electric Currents, and Heat Transfer interfaces domains. Specific materials are selected and assigned to each domain. For the Solid Mechanics interface, the anchors of the U-shaped structures, the flexure beams and one side of the microbeams are set with a fixed constraint. For the Electric Currents, an electric potential is applied on one of the anchors (A1, B1, C1, D1, and E1/E2) while others are connected to ground (A2, B2, C2, D2, and E1/E2). For the Heat Transfer, the thermal boundaries are set at ambient temperature at the bottom of the anchors, and the rest of the structure is set to a convective heat boundary condition, where the heat flux option is used for an external natural convection with air as an external fluid and a vertical wall of height 1 m. Tetrahedral elements are used as the element type to mesh the structure. We used 8800 elements, which have been proven to provide acceptable converged results in efficient time, and hence used for all the simulation results presented in this work.

A major parameter that can potentially limit the performance of an electrothermal actuator is temperature. To avoid the thermal silicon structure damage, the temperature should be lower than 1273 K [29]. The electrothermal simulation results of Case 5 show a maximum temperature of 531 K and a maximum displacement of 7.2 μm at V_{Th}= 8 V, Fig. 5.

The simulation results of the structure deformation and the resonance frequencies in the device are shown, respectively, in Figs 5 and 6 for the eight cases. Each stiffness element of the cases has a different value, which allows the possibility of achieving different mid-point deformation with the voltage. Fig. 5 shows the maximum displacement and von Mises stress of the mid-point arch microbeam for Case 7. In this case and at V_{Th}= 8 V, the

maximum displacement and von Mises stress are 16.4 μm and 56 Mpa, respectively. We can obtain the same displacement of 5.4 μm under V_{th}= 4.3 V, 5.5 V, 6 V, 7.1 V, 7.5 V, 7.6 V, and 8 V for cases: 8, 7, 0, 5, 2, 3 and 1, respectively. This indicates the possibility for compensating for the potential environmental effects that can cause changes of the device static behavior through changing the side-actuation and thermal voltages.

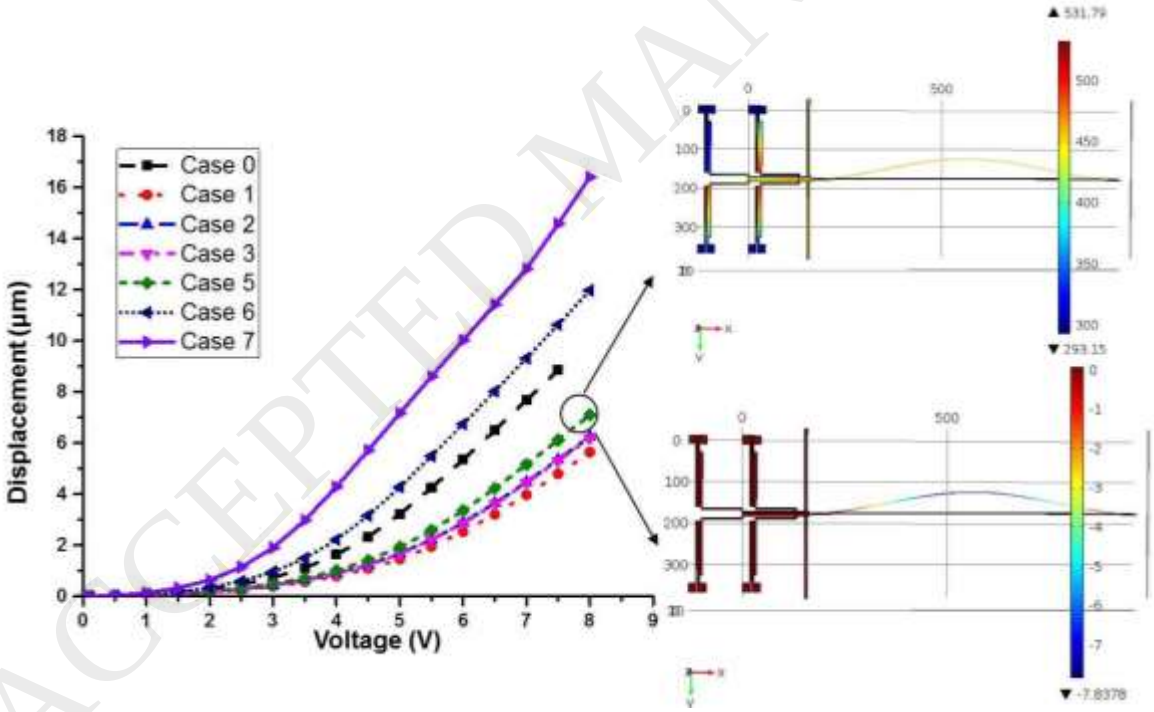

(a) (b)

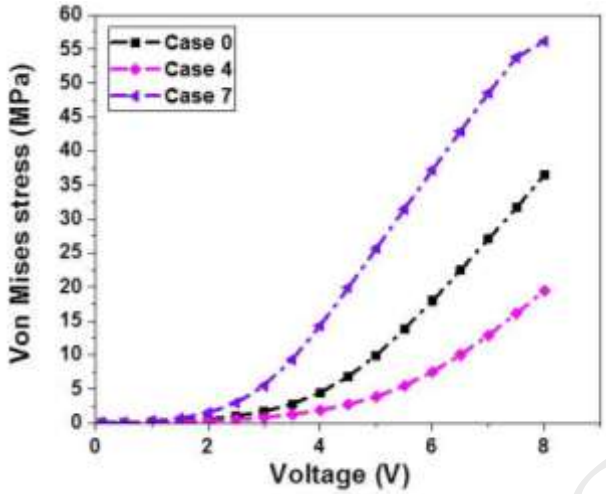

(c)

Fig. 5: (a) FE simulations showing the mid-point microbeam deformation as a function of V_{th} for the eight cases. (b) Temperature distribution in Kelvin (up right) and total displacement in micrometer (down) for case 5 at V_{Th}= 8 V. (c) Maximum von Mises stress at microbeam mid-point as a function of V_{th} for three selected cases.

In Fig. 6, it is observed that for all the cases, the electrothermal voltage leads to an initial decrease in the first resonance frequency until it reaches a critical point, after which it increases due to the increase in curvature level that dominates the compressive force effect. The third resonance frequency on the other hand shows continuous decrease. As shown in the figure, each stiffness element (case) results in a shifted frequency response curve. For instance, the curve inflection point at 3 V for Case 7 is shifted to 6.5 V for Case 2. We can obtain the same tuning at the inflection point under V_{th}=4V, 5.5 V, 5.5 V, 6 V, 6 V and 4.5 V for cases: 0, 5, 1, 3, 2 and 4, respectively. This again demonstrates a mechanism to compensate for the undesirable changes of the device dynamic behavior through changing the side-actuation and thermal voltages.

A wide tunability is shown for the first (Fig. 6(a)) and third (Fig. 6(b)) modes. This tunability depends on the electrothermal actuation configuration (the cases). Also, the results show the capability of shifting and choosing the operating frequency range upon demand.

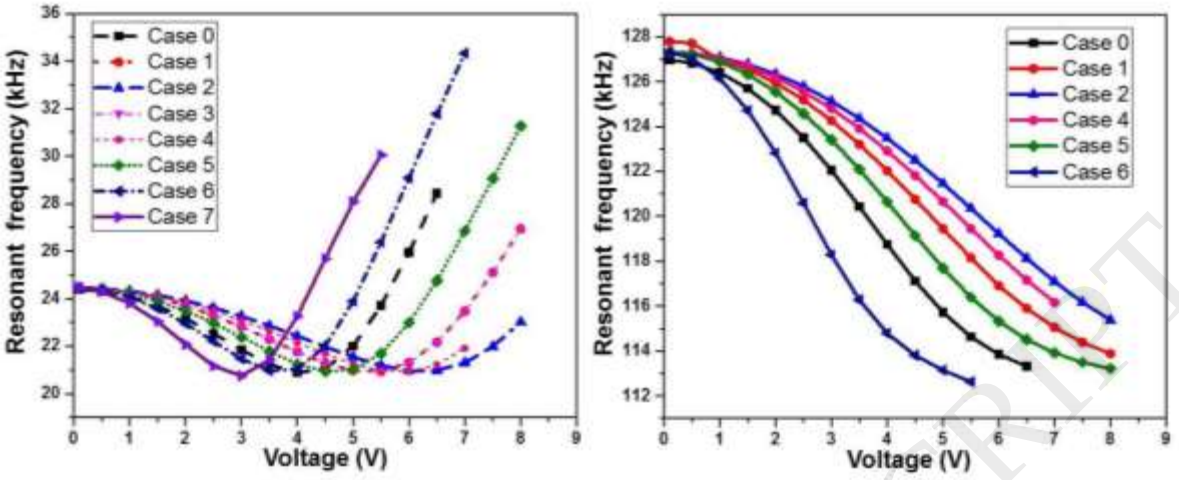

(a) (b)

Fig. 6: The simulated change in the resonance frequency with V_{th} for different cases for (a) the first resonant mode and (b) the third resonant mode.

5. Experimental results and discussion

To experimentally characterize the deflections as well as the resonance frequencies of the microbeam, we utilized a Micro System Analyzer (MSA-500) from Polytec with an in-plane dynamic measurement system using a stroboscopic video microscopy (Fig. 7). We used the ring down measurement and the Fast Fourier Transform (FFT) method to measure the resonance frequencies of the beams for each value of V_{th}, applied on the U–shaped structures. A topographical characterization is used to determine the static mid-point deflection of the microbeam.

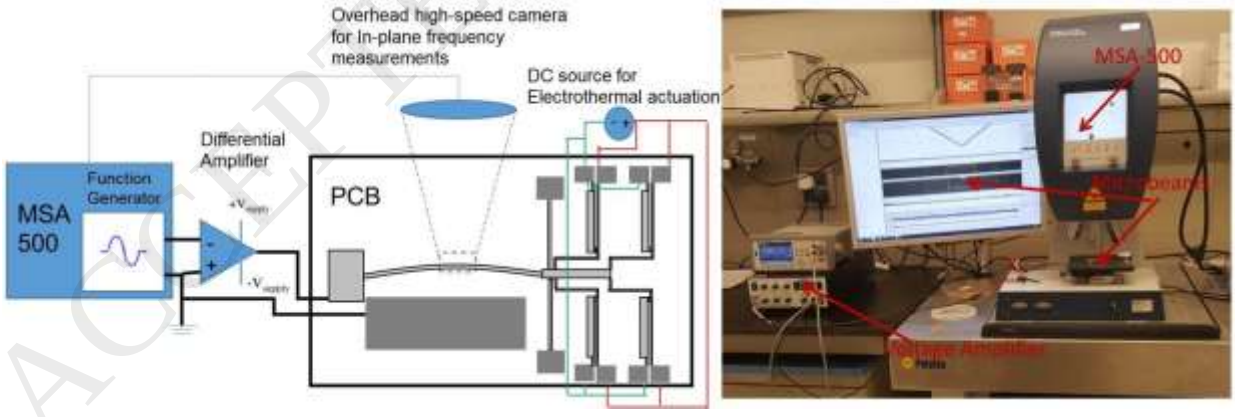

(a) (b)

Fig. 7: Experimental setup. (a) Schematic and (b) a picture.

The gap between the actuating electrode and the beam mid-point is 12.5μm, which restricts the maximum deflection that can be demonstrated. Thus, only the cases which have maximum mid-point displacement lower than 12.5μm can be shown. Fig. 8a shows the measured mid-point deflections of the microbeam for Case 0, Case 2, Case 3, and

Case 8. Case 8 corresponds to the electrical connection of A, B, and D. The figure shows four different beam responses for the four ways of electrothermal actuation. In agreement with the finite element simulations, the experimental results show Case 0 having a high displacement and low actuation voltage compared to the other cases. The experimental results illustrate that this micro actuator can move up to 8.3μm when applying an actuation voltage of 8.5 V (Case 2).

Figs. 8 (b) and (c) show the frequency responses of the microbeam. Fig. 8(b) shows seven values of the critical inflection points of the frequency response curve for all cases. The choice of the electrothermal configuration allows the possibility of shifting the inflection points and controlling the resonance frequencies. For resonators, it is desirable to have high tunability. As shown in the figure, for Case 0, the device indicates a high tunability estimated to be 73 % and 10 %, for the first and third modes. Also, at V_{th}= 7 V, the first and third resonance frequencies can be increased, respectively, from 22 kHz to 31 kHz and from 114.5 kHz to 121.8 kHz. The dynamic and the static results of such structure can be promising for many applications, such as filters, memory devices, and switches where large deflections and high tuning ranges are needed.

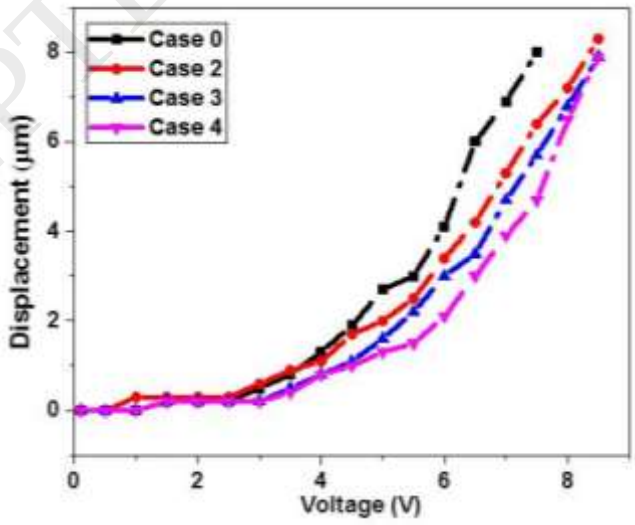

(a)

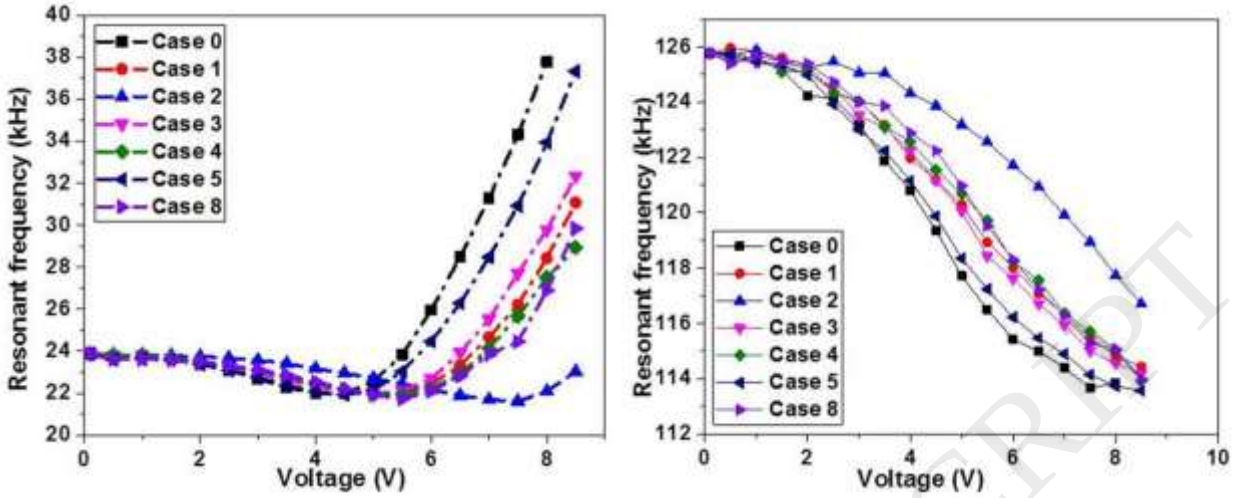

(b) (c)

Fig. 8: The measured mid-point deflection (a) and the resonance frequency with V_{th} for different cases for (b) the first resonant mode and (c) the third resonant mode.

The measured resonance frequencies and mid-point deflections of the microbeam are compared with the FE results in Fig. 9. One limitation of the used FE model is that the electrical and thermal parameters of the doped silicon are assumed constant while in general they are temperature dependent [30-31]. However, a good general agreement is shown among all results.

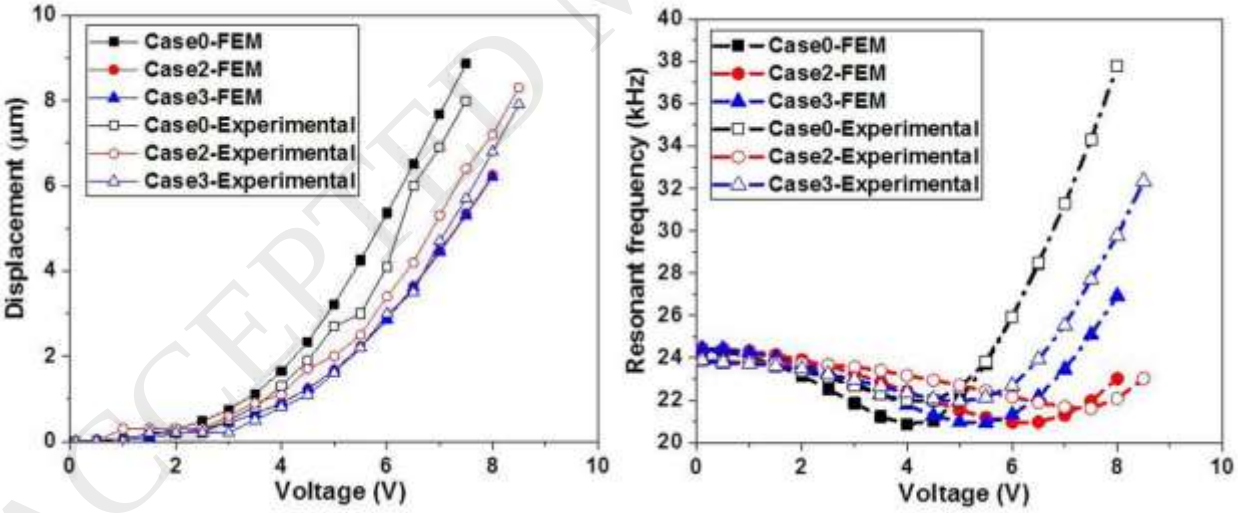

(a) (b)

Fig. 9: Measurements and FE simulations of (a) the mid-point deflection and (b) the resonance frequency of the first mode of the microbeam as varying V_{th}.

Based on the above figures, one can see that wide-range tunable resonator and high displacement actuators are demonstrated using finite element simulation and experimentally. Using electrothermally actuated MEMS clamped-

guided arch beams along with U-shaped thermal actuators have demonstrated the flexibility of shifting and choosing the operating frequency range upon demand; for both the first and third vibration modes. Next, we show how to use such high tunability to realize a dynamic electro-mechanical logic device.

6. Application : 2-bit logic functions

In this section, we demonstrate one potential application of the studied device to perform 2-bits logics functions, such as NOR, XOR, and AND, dynamically using the shift in its first mode frequencies. Such devices have been the subject of increasing interest in recent years [32-34]. Here, the high motional current of a capacitively sensed resonator is taken as output HIGH at resonance. Off resonance, the low state/output, and hence motional current, is taken as LOW.

To experimentally characterize the device, we utilized a network analyze (E5071C), Fig. 10(a). The arch microbeam is excited by an AC actuation signal from the network analyzer and then superimposed with a DC voltage to its lower electrode, which serves as the driving electrode. The output current induced at the sense electrode (upper electrode) is connected to a low-noise amplifier (LNA) with its output coupled to the network analyzer input port. The two U-shaped actuators are used as the logic inputs (V_A and V_B) and they are electrothermally actuated to control the resonance frequencies of the arch beam. The two inputs V_A and V_B are provided with two DC sources, which are used to switch between LOW and HIGH states of the S21 transmission. Fig. 10(b) shows the measured S21 transmission indicating resonances at f_0 = 14.876 kHz for V_A= V_B =0, f_1 = 14.624 kHz for (V_A= 3V, V_B =0) or (V_A= 0,V_B =3 V), and f_2 = 14.421 kHz for V_A= 3V, V_B = 3V).

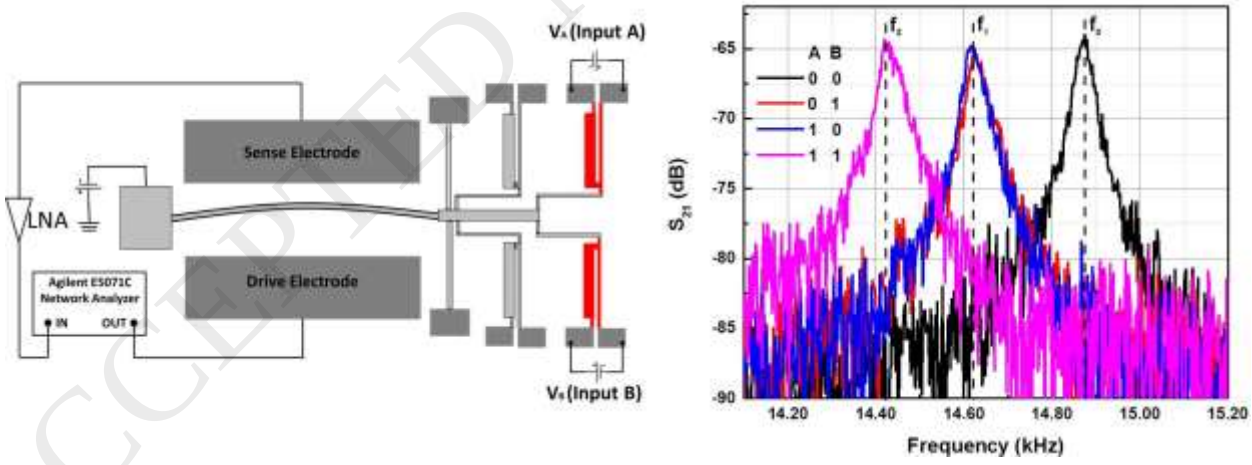

(a) (b)

Input A	Input B	NOR	XOR	AND
0	0	1	0	0
0	1	0	1	0
1	0	0	1	0
1	1	0	0	1

(c)

Fig. 10: (a) A schematic of the electrical experimental setup of the device. (b) Frequency responses of the arch beam at a 4.8 × 10^{-4} mbar pressure for the logic input conditions of (0,0), (0,1), (1,0), and (1,1), shown in black, blue, red, and magenta, respectively. (c) Logic functions operating NOR, XOR, and AND.

As shown in Fig. 10(b), the NOR logic operation is demonstrated when V_A= V_B =0 V, which corresponds to the resonance frequency f_0=14.876 kHz, where the S21 signal shows HIGH (black curve), denoted as logic output 1. For all other logic inputs, the S21 signal shows the level to be LOW, representing logic output 0. We apply the same principle to demonstrate the XOR logic operation, but in this case, one of the inputs is actuated at 3 V, which corresponds to the resonance frequency (f_1 =14.624 kHz), where the S21 signal shows HIGH (blue or red curves), denoted as logic output 1. For all other logic inputs, the S21 signal shows the level to be LOW, representing logic output 0. In the same way, the AND logic operation can be performed by applying V_A= V_B =3 V, which corresponds to the resonance frequency (f_2=14.876 kHz), where the S21 shows the HIGH level. The time response of the resonator showing the binary inputs A and B and the corresponding logic output is shown in Fig. 11

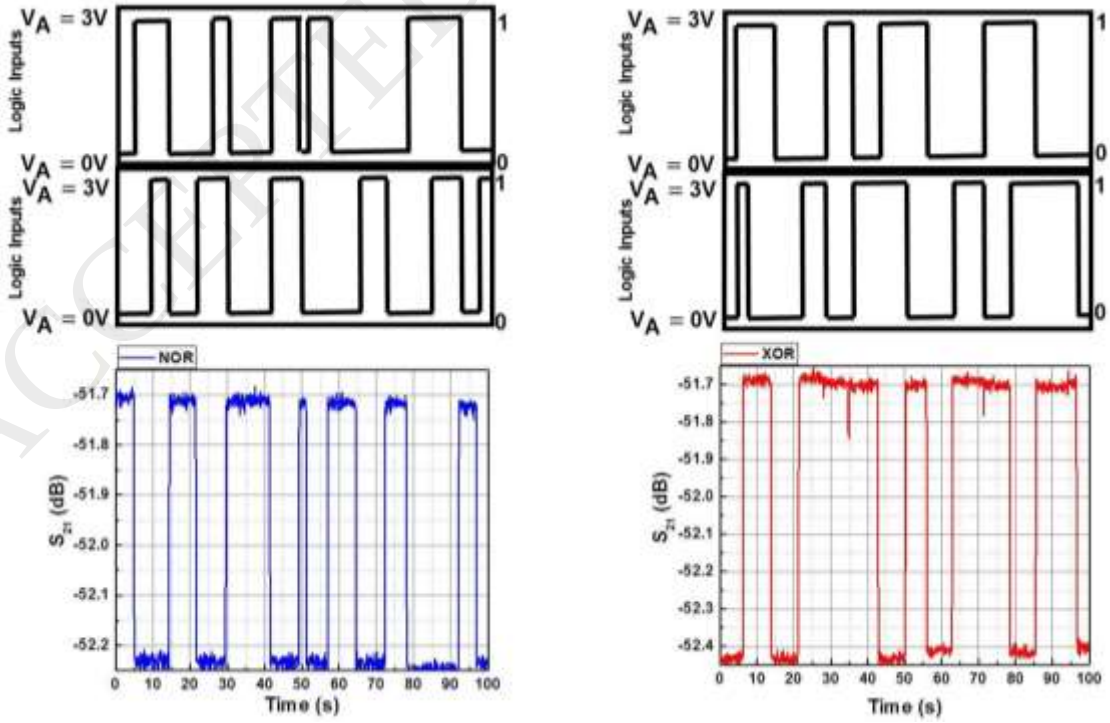

(a) (b)

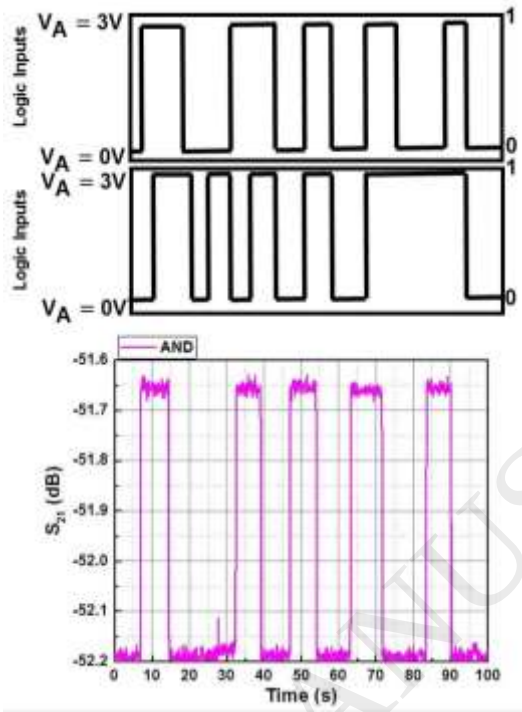

(c)

Fig. 11: Demonstration of logic operations (a) NOR, (b) XOR, and (c) AND, when V_A= 0 V and V_B =3 V, corresponding to 0 and 1 logic input conditions and S21 transmission signal corresponding to the logic output.

7. Conclusions

This paper presented an electrothermally structure, which combines U-shaped electrothermal actuators with in-plane arch clamped-guided microbeam. By varying the electrothermal voltage, the U-shaped structures are capable of producing multiway axial load on the guided microbeams, which serves as variable mechanical stiffness elements that control the axial displacement of the arch beams, their operating resonance frequency for the first and the third modes, and their static deflections. The devices were fabricated from a highly conductive silicon device layer of silicon-on-insulator (SOI) wafer. A multi-physics finite element model was utilized for the design and optimization. The finite element results demonstrate large displacement at moderate electrothermal voltage. The multi static response of the device and its ability to show high displacement, may lead to interesting possibilities in microactuator design. Through both the finite element simulations and the experimental results, we showed that the electrothermal voltage leads to initial decrease in the first resonance frequency until it reaches a critical point where the axial load effect dominates the response, in which case the resonance frequency increases until it saturates, while the third resonance frequency continues in decreasing. We showed that the resonance frequencies responses with electrothermally actuated voltage can be shifted and operated at a wide range of resonance frequency (73 %). In conclusion, we have demonstrated that it is possible to control the deflection and the resonance frequency of the

beam by employing different ways of electrothermal actuation. Also, we showed the capability of this structure to perform 2-bits logics functions, NOR, XOR, and AND.

Acknowledgment

This publication is based upon work supported by the King Abdullah University of Science and Technology (KAUST) office of sponsored research OSR under Award No. OSR-2016-CRG5-3001.

8. References

[1] D. Kim, E. Lee, M. Cho, C. Kim, Y. Park, T. Kouh, Pressure-sensing based on photothermally coupled operation of micromechanical beam resonator, Applied Physics Letters, 102 (2013) 203502.
[2] N. Jaber, A. Ramini, Q. Hennawi, M.I. Younis, Wideband MEMS resonator using multifrequency excitation, Sensors and Actuators A: Physical, 242 (2016) 140-145.
[3] M. Hajhashemi, A. Amini, B. Bahreyni, A micromechanical bandpass filter with adjustable bandwidth and bidirectional control of centre frequency, Sensors and Actuators A: Physical, 187 (2012) 10-15.
[4] B. Charlot, W. Sun, K. Yamashita, H. Fujita, H. Toshiyoshi, Bistable nanowire for micromechanical memory, Journal of Micromechanics and Microengineering, 18 (2008) 045005.
[5] M. Hafiz, L. Kosuru, M.I. Younis, Microelectromechanical reprogrammable logic device, Nature communications, 7 (2016) 11137.
[6] J. Moser, J. Güttinger, A. Eichler, M.J. Esplandiu, D. Liu, M. Dykman, A. Bachtold, Ultrasensitive force detection with a nanotube mechanical resonator, Nature nanotechnology, 8 (2013) 493-496.
[7] N. Krakover, B.R. Ilic, S. Krylov, Displacement sensing based on resonant frequency monitoring of electrostatically actuated curved micro beams, Journal of Micromechanics and Microengineering, 26 (2016) 115006.
[8] H. Ding, J. Zhao, B.-F. Ju, J. Xie, A high-sensitivity biaxial resonant accelerometer with two-stage microleverage mechanisms, Journal of Micromechanics and Microengineering, 26 (2015) 015011.
[9] N. Alcheikh, A. Ramini, M.A.A. Hafiz, M.I. Younis, Tunable Clamped–Guided Arch Resonators Using Electrostatically Induced Axial Loads, Micromachines, 8 (2017) 14.
[10] N. Alcheikh, A. Hajjaj, N. Jaber, M. Younis, Electrothermally actuated tunable clamped-guided resonant microbeams, Mechanical Systems and Signal Processing, 98 (2018) 1069-1076.
[11] U. Park, J. Rhim, J.U. Jeon, J. Kim, A micromachined differential resonant accelerometer based on robust structural design, Microelectronic Engineering, 129 (2014) 5-11.
[12] C. Zhao, G.S. Wood, J. Xie, H. Chang, S.H. Pu, M. Kraft, A force sensor based on three weakly coupled resonators with ultrahigh sensitivity, Sensors and Actuators A: Physical, 232 (2015) 151-162.
[13] T. Yang, R. Wiebe, Experimental Study on the Effect of Large Axial Tensile Force on the Natural Frequency of a Fixed-Fixed Steel Beam, Nonlinear Dynamics, Volume 1, Springer2017, pp. 127-134.
[14] T. Remtema, L. Lin, Active frequency tuning for micro resonators by localized thermal stressing effects, Sensors and Actuators A: Physical, 91 (2001) 326-332.
[15] A.Z. Hajjaj, N. Alcheikh, A. Ramini, M.A. Al Hafiz, M.I. Younis, Highly tunable electrothermally and electrostatically actuated resonators, Journal of Microelectromechanical Systems, 25 (2016) 440-449.
[16] A.Z. Hajjaj, A. Ramini, N. Alcheikh, M.I. Younis, Electrothermally Tunable Arch Resonator, Journal of Microelectromechanical Systems, (2017).
[17] R. Hickey, D. Sameoto, T. Hubbard, M. Kujath, Time and frequency response of two-arm micromachined thermal actuators, Journal of Micromechanics and Microengineering, 13 (2002) 40.
[18] J. Qiu, J.H. Lang, A.H. Slocum, A.C. Weber, A bulk-micromachined bistable relay with U-shaped thermal actuators, Journal of Microelectromechanical Systems, 14 (2005) 1099-1109.
[19] L. Que, J.-S. Park, Y.B. Gianchandani, Bent-beam electrothermal actuators-Part I: Single beam and cascaded devices, Journal of Microelectromechanical Systems, 10 (2001) 247-254.
[20] C. Guan, Y. Zhu, An electrothermal microactuator with Z-shaped beams, Journal of Micromechanics and Microengineering, 20 (2010) 085014.
[21] Y. Zhu, S.R. Moheimani, M.R. Yuce, Bidirectional electrothermal actuator with Z-shaped beams, IEEE Sensors Journal, 12 (2012) 2508-2509.

[22] M. Tecpoyotl-Torres, R. Cabello-Ruiz, J. G.Vera-Dimas, Design and simulation of an optimized electrothermal microactuator with Z-shaped beams. Acta Universitaria, 25(3).
[23] M.I. Younis, MEMS linear and nonlinear statics and dynamics, Springer Science & Business Media2011.
[24] D. Yan, A. Khajepour, R. Mansour, Design and modeling of a MEMS bidirectional vertical thermal actuator. Journal of Micromechanics and Microengineering, 14(7), 841.
[25] S.C. Masmanidis, R.B. Karabalin, I. De Vlaminck, G. Borghs, M.R. Freeman, M.L. Roukes, Multifunctional nanomechanical systems via tunably coupled piezoelectric actuation, Science, 317 (2007) 780-783.
[26] S.A. Tella, A.Z. Hajjaj, M.I. Younis, The effects of initial rise and axial loads on MEMS arches, Journal of Vibration and Acoustics, 139 (2017) 040905.
[27] MEMSCAP, SOIMUMPs, Durham, USA,2003, http://www.memscap.com/products/mumps/soimumps
[28] COMSOL Multiphysics User Guide, Version 4.3 a, COMSOL, AB: Burlington. MA, USA. https://www.comsol.com/
[29]HICKEY, M. Khujath, and T. Hubbard, "Heat transfer analysis and optimization of two-beams of Microelectromechanical thermal actuators," Journal of Vacuum Science and Technology A: Vacuum, Surfaces, and Films
[30] A.A. Geisberger, N. Sarkar, M. Ellis, G.D. Skidmore, Electrothermal properties and modeling of polysilicon microthermal actuators, Journal of Microelectromechanical Systems, 12 (2003) 513-523.
[31] C.D. Lott, T.W. McLain, J.N. Harb, L.L. Howell, Modeling the thermal behavior of a surface-micromachined linear-displacement thermomechanical microactuator, Sensors and Actuators A: Physical, 101 (2002) 239-250.
[32] I. Mahboob, E. Flurin, K. Nishiguchi, A. Fujiwara, H. Yamaguchi, Interconnect-free parallel logic circuits in a single mechanical resonator, Nature communications, 2 (2011) 198.
[33] M. Mita, M. Ataka, H. Toshiyoshi, Microelectromechanical XNOR and XOR logic devices, IEICE Electronics Express, 10 (2013) 20130187-20130187.
[34] A. Yao, T. Hikihara, Logic-memory device of a mechanical resonator, Applied Physics Letters, 105 (2014) 123104.

Nouha Alcheikh was born in 1984. She received her MS degree in electronics from the Polytechnic National Institute of Grenoble in 2007 and her PhD degree in RF MEMS from Grenoble University, France in 2011. From 2011 to 2014, she was as a Post-Doctoral fellow working on Force Sensors and Energy Harvesting at CEA-Leti/MINATEC Campus, Grenoble (France) and at IMS, Bordeaux (France). Since 2015, she has been a Post-Doctoral Fellow at King Abdullah University of Science and Technology, Thuwal, Saudi Arabia where she is performing her research on MEMS Sensors and Actuators,

Sherif Tella Sherif Tella received his ND (National Diploma) in Mechanical Engineering from Yaba College of Technology, Nigeria in 2005 and B.Sc degree in Mechanical Engineering from Obafemi Awolowo University, Nigeria in 2010. Then, He was awarded with MSc. with Distinction in Mechatronics from University of Glasgow, Glasgow, UK in 2014. He is currently enrolled as PhD student in Mechanical Engineering in KAUST. His research interests include dynamics and control of linear and nonlinear systems in MEMS and NEMS devices with applications in logics, memory, filters etc. He was

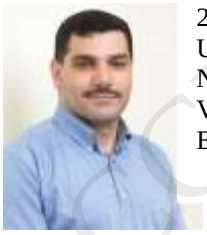

Mohammad I. Younis received a Ph.D. degree in engineering mechanics from Virginia Tech in 2004. He is currently an Associate Professor of Mechanical Engineering with King Abdullah University of Science and Technology, Saudi Arabia. He serves as an Associate Editor of Nonlinear Dynamics, the Journal of Computational and Nonlinear Dynamics, and the Journal of Vibration and Control. He is a member of IEEE and the American Society of Mechanical Engineers ASME.